On-Campus Over-the-Air Millimeter-Wave Channel Evaluation for Connected and Automated Mobility

Erik Kampert*, E. I. Adegoke*, Reiner Stuhlfauth†, Matthew D. Higgins*
*WMG, University of Warwick, Coventry, United Kingdom, e.kampert@warwick.ac.uk
†Rohde & Schwarz International GmbH, Munich, Germany

***Abstract*—High throughput wireless communication between vehicles and infrastructure will rely on millimeter-wave carriers and technology, which provide access to large bandwidths whilst still being able to establish stable links over distances of hundreds of meters. The work presented here, evaluates the quality of such signals in a mini-urban campus environment, by comparing detailed channel sounding results with signal quality parameters such as the error vector magnitude and the established data throughput. This provides insights into the relationships between fundamental parameters used to establish channel models and the quality of service parameters used in applications and standards. For the environment investigated, a strong threshold dependence of the signal quality on the received power is observed and explained in detail.**

***Index Terms*—Autonomous vehicles, millimeter-wave propagation, performance evaluation, radio link, vehicular communications.**

I. Introduction

Future personal mobility is developing towards Connected and Automated Mobility (CAM) solutions which include intelligent and self-driving vehicles, with a large research and engineering community investigating and overcoming the technical challenges in their development [1]. Although safest CAM solutions are expected to be fully self-supporting and autonomous, the ability to share and receive information from other vehicles or infrastructure holds promise to lead to advanced traffic and environment awareness as well as cooperative behaviour functions [2]. Modern vehicular communications cover an ever-growing range of techniques, use cases, and technical and legal Third Generation Partnership Project (3GPP) standards, from which it can benefit through effective multi-connectivity management [3], [4]. Of particular future potential is the addition of millimeter-wave (mmWave) technology, which makes use of the larger bandwidths available in the less congested radio frequency (RF) spectrum between 30 and 300 GHz. This allows for multi-gigabit per second data transfer, supporting the low-latency sharing of raw automotive perception sensor data between vehicles (e.g. from HD cameras and LiDAR scanners) or the uploading of all sensor data to the cloud for further off-board processing and analysis. As antenna apertures scale with the used wavelength, mmWave antennas benefit from their compactness and thus possibility to be embedded inside vehicles, as well as the potential to be combined in relatively small antenna arrays that allow for antenna beam switching, steering and tracking [5], [6]. A drawback of individual mmWave antennas is their small effective area compared to antennas for communication below $7.125\,\mathrm{GHz}$, which is solely responsible for the perceived frequency dependence of the path loss in an end-to-end radio channel. Combined with the higher absorption of mmWave radiation by materials, this makes the mmWave communication channel more susceptible to obscurations and blockages. For effective long distance communication over hundreds of meters, this basically requires a direct line-of-sight (LOS) connection.

The work presented here, therefore, experimentally investigates mmWave channel sounding parameters (such as path loss and delay spread) for a Vehicle-to-Infrastructure (V2I) communication channel in a mini-urban university campus environment. Furthermore, it relates the results to the associated measured channel evaluation parameters; Error Vector Magnitude (EVM) and data throughput for the same communication path. Whereas mmWave path loss models have been designed for various environments based on empirical and simulation work, the novelty in this work lies in the direct comparison with the communication channel's Quality of Service (QoS) indicator EVM and its achievable data throughput [7], [8]. For measuring the QoS parameter throughput, which is a performance indicator, typically an end-to-end data connection is required. EVM permits the a-priori estimation of the achievable throughput without the need for a full protocol stack. For this particular study, the focus is on the 3GPP band n257 and using a carrier frequency of 28.5 GHz, as a representative of the prioritised first high frequency band for 5G [9].

II. Experimental Details

A. Environment

Extending the acquired knowledge from channel sounding and evaluation measurements performed inside anechoic chambers, the evaluation of outdoor V2I performance adds realism to the tested scenarios. Moreover, such results can then be used to validate and optimise the current channel models based on stochastic and deterministic methods [10], [11]. The specific scenario of interest is the communication path from an enclosed pedestrian bridge that connects the second floors of two departmental buildings on the University of Warwick's central campus (the International Manufacturing Centre and the Energy Innovation Centre) to the pavement along Lord Bhattacharyya Way towards the National Automotive Innovation Centre (NAIC). Within the Midlands Future Mobility CAM Testbed, this road is part of a route on which swarming autonomous pods are to be deployed [12], [13]. Hence, the presented results can be combined with previous work regarding the channel evaluation of such pods, in order to provide a detailed understanding of the potential of 5G V2I communication in this scenario [14]. Furthermore, the work presented here can also be extended with recent outdoor measurements in the 5G New Radio Frequency Range 1 (5G NR FR1), for a connected pod route in a more open urban environment [15]. The transmitting antenna (TX) location is approximately $8.3\,\mathrm{m}$ above the pavement and slightly offset from the centre of the road, at $2.4\,\mathrm{m}$ distance from the line along which the receiving antenna (RX) is moved on the pavement. The RX is positioned at a height of $1.2\,\mathrm{m}$, is moved to various positions on the pavement alongside Lord Bhattacharyya Way, and is boresight aligned with the TX. Fig. 1 displays the boresight views of the TX and RX for selected antenna locations.

B. Channel Sounding

The WMG channel sounding equipment uses the pulse compression method and consists of an R&S SMW200A Vector Signal Generator, an R&S FSW85 Signal and Spectrum Analyzer and an R&S RTO2044 Digital Oscilloscope, and has been described in our previous work [16]. For the channel sounding experiments the Frank–Zadoff–Chu (FZC) waveform is generated at a fixed RF output power of $20\,\mathrm{dBm}$, and the excess loss and root-mean-square delay spread values are determined from the received signal. Dividing the received power by $400\,\mathrm{MHz}$, the largest foreseen channel bandwidth for 5G New Radio Frequency Range 2 (5G NR FR2), results in the representative Received Power Spectral Density (RPSD) [17]. Both the TX and RX are connected to their respective ends of the channel sounding equipment with $2\,\mathrm{m}$ long, low loss, phase-stable coaxial cables, which have a typical insertion loss of $4.8\,\mathrm{dB}$ each, plus $0.5\,\mathrm{dB}$ from a between-series coaxial adapter matching the input connector of the FSW85.

C. Channel Evaluation with mmWave Transceiver System

The channel evaluation experiments are carried out using the NI mmWave Transceiver System (MTS), which is a software-defined radio with $2\,\mathrm{GHz}$ real-time bandwidth. The MTS is based on a multi-FPGA processing architecture, which enables it to both capture and generate $2\,\mathrm{GHz}$ of data and process these in real time. This setup has been described in detail in our previous work [14]. Shortest possible, low loss, phase-stable coaxial cables are used for the channel evaluation measurements in order to have access to the highest possible TX output and RX input power, thereby establishing the largest possible range for a high-throughput communication link. These cables are $30\,\mathrm{cm}$ and $65\,\mathrm{cm}$ long and have a typical insertion loss of $1.0\,\mathrm{dB}$, respectively $1.7\,\mathrm{dB}$.

III. Results and Discussion

A. Channel Sounding

In order to enable the largest possible communication range for a high-order QAM modulation scheme, two waveguide horn antennas with a typical gain of $25\,\mathrm{dBi}$ and a half-power beam width (HPBW) of $10°$ are used as both the TX and RX. Because of live traffic on the road and pedestrians on the pavement, the measurement duration is adapted such that related obstruction effects can be distinguished from obscuring effects due to the stationary communication path, which are of primary interest. Fig. 2 (a) and (b) display the RPSD and excess loss (EL) for various antenna separations, ranging from 13 to $308\,\mathrm{m}$. EL is calculated based on the difference between the received power P_{RX}, the transmitted power P_{TX}, the transmitter and receiver antenna gains G_{TX} and G_{RX}, the

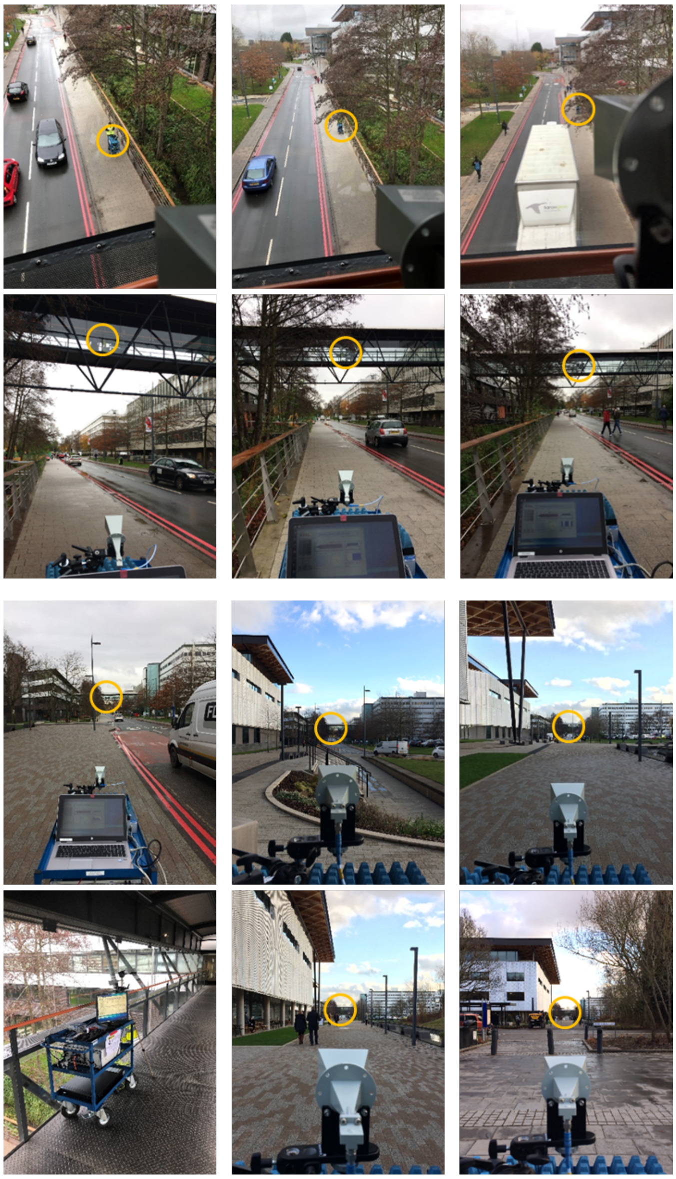

Fig. 1. Photos of the V2I channel evaluation measurements from the pedestrian bridge between the IMC and EIC-buildings to the pavement along the Lord Bhattacharyya Way, varying the line-of-sight distance between the TX and RX from 13 to 23, 34, 100, 165, 208, 256 and $308\,\mathrm{m}$ (first row: TX boresight view, RX encircled; second, third and fourth row: RX boresight view, TX encircled). Waveguide horn antennas with a typical gain of $25\,\mathrm{dBi}$ and a HPBW of $10°$ are used as both the TX and RX.

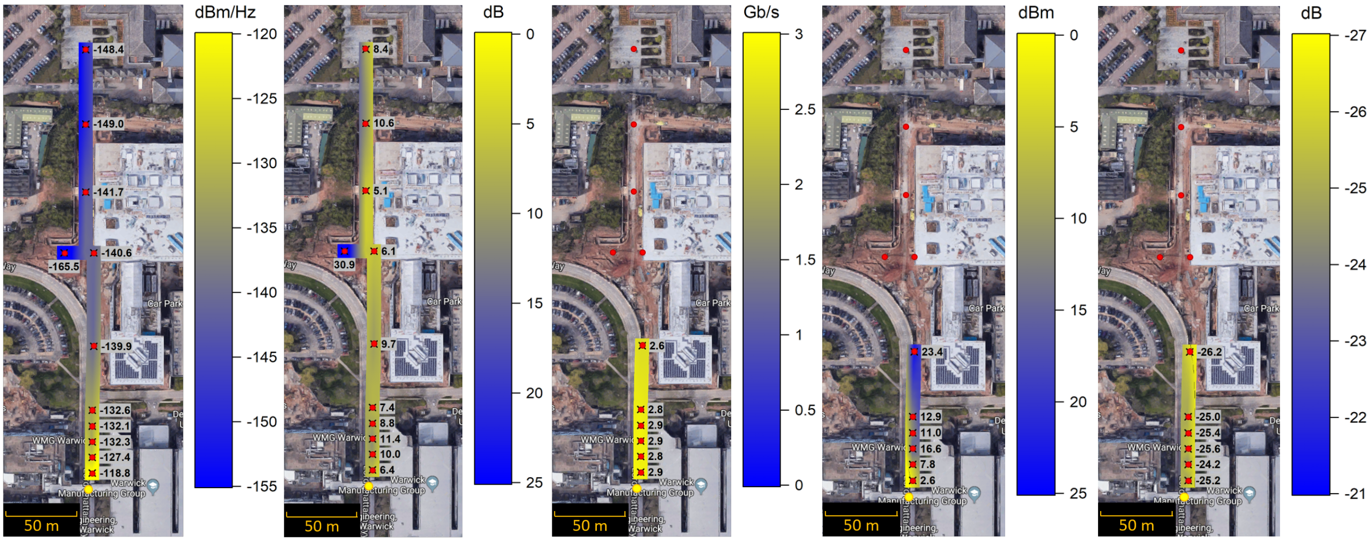

(a) RPSD (b) Excess loss (c) Throughput (d) Minimum P_{TX} (e) EVM

Fig. 2. (a) Received Power Spectral Density at various locations along the Lord Bhattacharyya Way with the transmitter located $8.3\,\mathrm{m}$ above the pavement and output power P_{TX} = $20\,\mathrm{dBm}$. The receiver is positioned $1.2\,\mathrm{m}$ above the pavement and its location is step-wise varied (red dots). The measured values (grey boxes) are converted into a contour plot through triangulation, interpolation and smoothing to visualise the highly likely in-between trend. Waveguide horn antennas with a typical gain of $25\,\mathrm{dBi}$ and HPBW of $10°$ are used as both TX and RX. (b) Excess loss with respect to free space path loss for the same locations. (c) Maximum achievable throughput for minimum required P_{TX}. (d) Minimum required P_{TX} to achieve the maximum throughput at a certain location. (e) Error Vector Magnitude corresponding with the maximum achievable throughput in (c) and the minimum required P_{TX} in (d). Background images were obtained from Google Maps.

transmitter and receiver losses L_{TX} and L_{RX}, and the free space path loss (FSPL) that depends on the antenna separation d, the carrier frequency f, and the speed of light in vacuum c, following

$$\mathrm{EL}(f)[\mathrm{dB}] = P_{RX} - P_{TX} + G_{TX}(f) + G_{RX}(f) - L_{TX}(f) - L_{RX}(f) - 20\log_{10}\left(\frac{4\pi d f}{c}\right) \quad (1)$$

As has been reported previously, an extensive set-up calibration simplifies (1) to [16]

$$\mathrm{EL}(f)[dB] = P_{RX} - \mathrm{cal}(f) - 20\log_{10}(d) \quad (2)$$

The use of FSPL, equal to a path loss exponent of 2, is justified here through the dominant LOS environment, and is further supported by ray tracing simulations for mmWave V2I communication in a comparable urban canyon environment [11]. As the focus of this paper is on the impact of the campus environment on the mmWave V2I QoS, the effects of the exact path loss exponent on the EL calculation are of minor importance, as they are included in the RPSD.

The obtained EL values in Fig. 2 (b) vary only slightly with the RX location as the LOS paths are mostly unobscured. Therefore, the contour plot displays little colour variation, except for the most left RX location in which a row of trees almost completely blocks the mmWave signal. From the EL values for short LOS paths, it is concluded that the absorption of the thick glass windows of the pedestrian bridge is relatively high, possibly up to $6\,\mathrm{dB}$. Additional verification measurements are planned to determine the exact loss contribution of the windows, which can then be included in L_{TX} in (1) and subsequently in cal(f) in (2), and subtracted from the current results.

B. Link Performance

Using the MTS, the TX power is varied for all antenna constellations on the path displayed on the photos of Fig. 1 up to an antenna separation of $100\,\mathrm{m}$, and the EVM and data throughput are recorded. As the aim is to achieve maximum data throughput, a 64-QAM scheme with a 7/8 code rate is chosen, resulting in a maximum throughput of $2.867\,\mathrm{Gb/s}$. This choice also determines the maximum TX-RX separation over which a stable, full throughput link can be established, as the modulation scheme affects the required EVM and thus the associated RPSD [14], [17]. For the environment investigated, the range for the present set-up and settings is limited to $\sim 100\,\mathrm{m}$.

Fig. 3 displays selected raw EVM and data throughput measurement results for two specific TX-RX separations. At an antenna separation of $13\,\mathrm{m}$, the antenna boresight views are clear and the measurement results show a gradually decreasing EVM with decreasing P_{TX}, combined with a threshold in the data throughput for an EVM between -23 and $-25\,\mathrm{dB}$. At an antenna separation of $34\,\mathrm{m}$, the boresight views are partly obscured by the branches of a tree next to the pavement (see Fig. 1, centre of the top row). Hence, a much larger P_{TX} is required to obtain a certain throughput. Moreover, a large time-dependent signal variation is observed, if the throughput

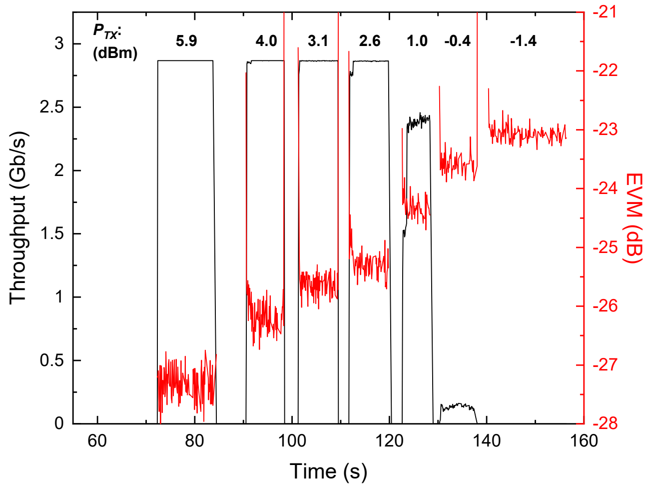

(a) TX-RX separation = $13\,\mathrm{m}$

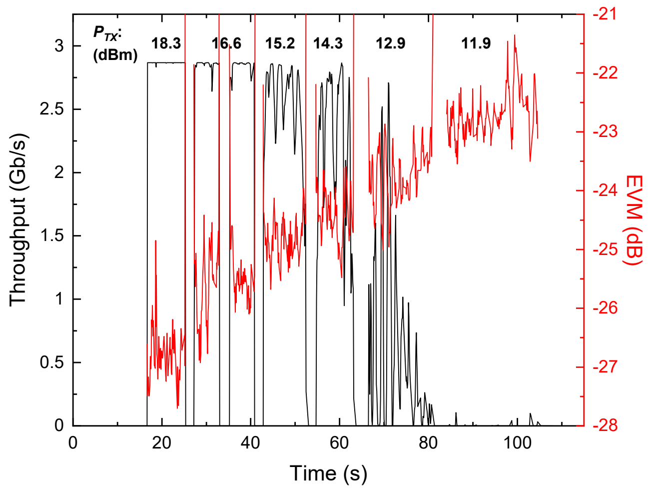

(b) TX-RX separation = $34\,\mathrm{m}$

Fig. 3. Plots of the measured data throughput and EVM values for the V2I channel from the pedestrian bridge between the IMC and IEC-buildings to the pavement along the Lord Bhattacharyya Way, for (a) a $13\,\mathrm{m}$ and (b) a $34\,\mathrm{m}$ antenna separation. For a carrier frequency of $28.5\,\mathrm{GHz}$ and a bandwidth of $800\,\mathrm{MHz}$, the unaveraged measured throughput (black, left y-axis) and EVM (red, right y-axis) are plotted versus time, stepwise varying P_{TX} (see top of plots). The modulation scheme is 64-QAM with a code rate of 7/8.

is neither zero nor maximum. This is most likely due to the branches of the tree moving in weak wind, that change the path obscuration, which highlights the strong effects that small changes in received RF power can have on the QoS, if the RPSD is close to the threshold below which EVM rapidly deteriorates.

In Fig. 2 (c), for TX-RX separations ranging from 13 to $100\,\mathrm{m}$, and P_{TX} varying from 2 to $24\,\mathrm{dBm}$ accordingly, a maximum data throughput of $\sim$2.6-2.8 $\mathrm{Gb/s}$ can be observed for all positions. Associated with the recorded maximum data throughput for all positions, Fig. 2 (e) displays EVM values of approximately $-25\,\mathrm{dB}$, achieved for a minimum RPSD range from -136 to $-140\,\mathrm{dBm/Hz}$, in line with 3GPP specifications and previous observations. Fig. 2 (d) provides details of the minimum required P_{TX} for the maximum data throughput as achieved in Fig. 2 (c). These values follow the RPSD obtained in the channel sounding experiments, confirming the expected linear dependence between transmitted and received power. Taking into account the previously mentioned, potentially high absorption of the pedestrian bridge's windows, if the TX would be mounted at the bridge's exterior, full throughput could be achieved up to the west facade of the NAIC-building at $\sim$$200\,\mathrm{m}$. This should lead to a minimum required RPSD of -136 dBm/Hz that allows full throughput in a 64-QAM modulation scheme. From the channel sounding results it could additionally be observed, that multipath components via nearby buildings and street furniture only become apparent at TX-RX separations larger than $250\,\mathrm{m}$, which then increase the delay spread and thereby the intersymbol interference probability, which could further negatively affect the EVM.

IV. Conclusions

Through a combination of channel sounding and channel evaluation measurements, this work links fundamental properties of mmWave V2I channels with signal quality properties on which applications rely. From the presented on-campus measurements, the crucial dependence on LOS paths between the transmitter and receiver, and the actual received signal power become apparent. Future work will extend the presented scenario to campus road crossings and pedestrianised areas using other suitable elevated TX locations. Moreover, using antennas with a larger HPBW in these scenarios could provide further insights into the potential effects of multipath components on the QoS. Combined with an additional study on the modulation scheme dependence, this would contribute to an in-depth understanding of the implications of both infrastructure and vehicular antenna choice and location for mmWave V2I communication.

Acknowledgment

This work was supported in part by the WMG Centre High Value Manufacturing Catapult, University of Warwick, Coventry, U.K., in part by the Wireless Infrastructure Group, Bellshill, U.K., in part by Midlands Future Mobility, University of Warwick, Coventry, U.K, and in part by the EPSRC through the UK-RAS Network.

References

[1] S. Coicheci and I. Filip, "Self-driving vehicles: current status of development and technical challenges to overcome," in *2020 IEEE 14th International Symposium on Applied Computational Intelligence and Informatics (SACI)*, 2020, pp. 000 255–000 260.

[2] J. He, Z. Tang, X. Fu, S. Leng, F. Wu, K. Huang, J. Huang, J. Zhang, Y. Zhang, A. Radford, L. Li, and Z. Xiong, "Cooperative Connected Autonomous Vehicles (CAV): Research, Applications and Challenges," in *2019 IEEE 27th International Conference on Network Protocols (ICNP)*, 2019, pp. 1–6.

[3] Z. Jako, A. Knap, L. Nagy, and A. Kovacs, "Vehicular communication – a technical overview," in *Cooperative Intelligent Transport Systems: Towards high-level automated driving*, ser. Transport, M. Lu, Ed. Institution of Engineering and Technology, 2019, pp. 135–159. [Online]. Available: https://digital-library.theiet.org/content/books/10.1049/pbtr025e_ch7

[4] A. Kousaridas, C. Zhou, D. Martín-Sacristán, D. Garcia-Roger, J. F. Monserrat, and S. Roger, "Multi-Connectivity Management for 5G V2X Communication," in *2019 IEEE 30th Annual International Symposium on Personal, Indoor and Mobile Radio Communications (PIMRC)*, 2019, pp. 1–7.

[5] K. Heimann, J. Tiemann, D. Yolchyan, and C. Wietfeld, "Experimental 5G mmWave Beam Tracking Testbed for Evaluation of Vehicular Communications," in *2019 IEEE 2nd 5G World Forum (5GWF)*, 2019, pp. 382–387.

[6] Y. Zhou, V. Basavarajappa, S. Alkaraki, and Y. Gao, "28 GHz Millimeter Wave Multibeam Antenna Array with Compact Reconfigurable Feeding Network," in *2020 14th European Conference on Antennas and Propagation (EuCAP)*, 2020, pp. 1–4.

[7] I. A. Hemadeh, K. Satyanarayana, M. El-Hajjar, and L. Hanzo, "Millimeter-Wave Communications: Physical Channel Models, Design Considerations, Antenna Constructions, and Link-Budget," *IEEE Communications Surveys Tutorials*, vol. 20, no. 2, pp. 870–913, 2018.

[8] R. A. Shafik, M. S. Rahman, A. R. Islam, and N. S. Ashraf, "On the error vector magnitude as a performance metric and comparative analysis," in *2006 International Conference on Emerging Technologies*, 2006, pp. 27–31.

[9] "Commission Implementing Decision (EU) 2019/784 of 14 May 2019 on harmonisation of the 24.25-27.5 GHz frequency band for terrestrial systems capable of providing wireless broadband electronic communications services in the Union," *Official Journal of the European Union*, vol. L 127, pp. 13–22, 2019. [Online]. Available: https://eur-lex.europa.eu/legal-content/EN/TXT/PDF/?uri=CELEX:32019D0784&from=EN

[10] M. Ozpolat, O. Alluhaibi, E. Kampert, and M. D. Higgins, "Connectivity Analysis for mmWave V2V Networks: Exploring Critical Distance and Beam Misalignment," in *2019 IEEE Global Communications Conference (GLOBECOM)*, 2019, Conference Proceedings, pp. 1–6.

[11] D. He, L. Wang, K. Guan, B. Ai, J. Kim, and Z. Zhong, "Channel Characterization for mmWave Vehicle-to-Infrastructure Communications in Urban Street Environment," in *2019 13th European Conference on Antennas and Propagation (EuCAP)*, 2019, pp. 1–5.

[12] [Online]. Available: https://midlandsfuturemobility.co.uk

[13] R. Woodman, W. Hill, S. Birrell, and M. D. Higgins, "An Evolutionary Approach to the Optimisation of Autonomous Pod Distribution for Application in an Urban Transportation Service," in *2019 23rd International Conference on Mechatronics Technology (ICMT)*, 2019, pp. 1–6.

[14] E. Kampert, C. Schettler, R. Woodman, P. A. Jennings, and M. D. Higgins, "Millimeter-Wave Communication for a Last-Mile Autonomous Transport Vehicle," *IEEE Access*, vol. 8, pp. 8386–8392, 2020.

[15] E. I. Adegoke, E. Kampert, and M. D. Higgins, "Channel Modeling and Over-the-Air Signal Quality at 3.5 GHz for 5G New Radio," *IEEE Access*, vol. 9, pp. 11 183–11 193, 2021.

[16] E. Kampert, P. A. Jennings, and M. D. Higgins, "Investigating the V2V Millimeter-Wave Channel Near a Vehicular Headlight in an Engine Bay," *IEEE Communications Letters*, vol. 22, no. 7, pp. 1506–1509, 2018.

[17] 3GPP, "Technical Specification Group Radio Access Network; NR; User Equipment (UE) radio transmission and reception; Part 2: Range 2 Standalone (Release 16)," 3rd Generation Partnership Project, Technical Specification (TS) 38.101-2, 2020-09, version 16.5.0. [Online]. Available: https://www.3gpp.org/ftp//Specs/archive/38_series/38.101-2/38101-2-g50.zip